Spindle Dynamics during Meiosis in *Drosophila* Oocytes

Sharyn A. Endow and Donald J. Komma

Department of Microbiology, Duke University Medical Center, Durham, North Carolina 27710

Abstract. Mature oocytes of *Drosophila* are arrested in metaphase of meiosis I. Upon activation by ovulation or fertilization, oocytes undergo a series of rapid changes that have not been directly visualized previously. We report here the use of the Nonclaret disjunctional (Ncd) microtubule motor protein fused to the green fluorescent protein (GFP) to monitor changes in the meiotic spindle of live oocytes after activation in vitro. Meiotic spindles of metaphase-arrested oocytes are relatively stable, however, meiotic spindles of in vitro–activated oocytes are highly dynamic: the spindles elongate, rotate around their long axis, and undergo an acute pivoting movement to reorient perpendicular to the oocyte surface. Many oocytes spontaneously complete the meiotic divisions, permitting visualization of progression from meiosis I to II. The movements of the spindle after oocyte activation provide new information about the dynamic changes in the spindle that occur upon re-entry into meiosis and completion of the meiotic divisions. Spindles in live oocytes mutant for a loss-of-function *ncd* allele fused to *gfp* were also imaged. The genesis of spindle defects in the live mutant oocytes provides new insights into the mechanism of Ncd function in the spindle during the meiotic divisions.

Meiosis is a specialized cell division that results in the formation of haploid gametes instead of diploid daughter cells, as in mitosis. Special features of meiosis that differ from mitosis include pairing of homologous chromosomes, recombination between homologues, and the occurrence of two successive divisions that reduce the chromosomes to the haploid number. Oocytes of most organisms are arrested at specific stages of meiosis that differ depending on the organism and can be activated by ovulation or fertilization to re-enter the cell cycle and complete the meiotic divisions.

Insights into the regulation of meiosis are anticipated to come from an understanding of the assembly, arrest, and reactivation of the meiotic spindle. Several structural differences exist between meiotic spindles of some oocytes and mitotic spindles of most animal cells. A striking difference is the absence of centrosomes at spindle poles of oocytes of several organisms that have been examined, including *Drosophila* (Sonnenblick, 1950), *Xenopus* (Gerhart, 1980), and the mouse (Szollosi et al., 1972). The absence of centrosomes raises the question of how microtubules are nucleated and organized for assembly of these spindles.

Thin-section electron microscopy has demonstrated that meiotic spindles of mouse oocytes lack centrosomes and centrioles, but electron-dense foci of microtubules are present at the broad poles of the oocyte spindles (Szollosi et al., 1972). A centrosomal protein, pericentrin, has been localized to multiple foci at the poles of the mouse oocyte spindle (Doxsey et al., 1994), consistent with the interpretation that the foci constitute dispersed microtubule organizing centers. Assembly of the meiotic spindle could occur from these dispersed centers in a manner similar to that of a single center. In contrast, known centrosomal components have not been identified in the *Drosophila* meiosis I spindle and are thought to be absent. The centrosomal protein, DMAP190 (CP190), was not found at the poles of the meiosis I spindle (Theurkauf and Hawley 1992), but it has recently been reported to localize to a ring- or disk-shaped structure between the two tandem meiosis II spindles of *Drosophila* oocytes (Riparbelli and Callaini, 1996). The ring-shaped structure in the central pole region of the *Drosophila* meiosis II spindles was observed previously (Puro, 1991) and was suggested to function in pole organization for the second meiotic division. Nucleation and organization of microtubules for assembly of the *Drosophila* meiosis I and II spindles could therefore differ from one another and from anastral spindles of other organisms.

The discovery that several of the recently identified kinesin microtubule motor proteins are spindle-associated has led to the hypotheses that the kinesin motors function to generate the forces required for spindle assembly and maintenance of spindle bipolarity (for review see Walczak and Mitchison, 1996). *Drosophila* Nonclaret disjunctional (Ncd;[1] Yamamoto et al., 1989; Endow et al., 1990; McDonald and

Please address all correspondence to Sharyn A. Endow, Department of Microbiology, Duke University Medical Center, Durham, NC 27710. Tel.: (919) 684-4311; Fax: (919) 684-8735; E-mail: endow@galactose.mc.duke.edu

1. *Abbreviations used in this paper*: *blo*, bloated; *ca*nd, claret nondisjunctional; GFP, green fluorescent protein; Ncd, Nonclaret disjunctional; *so*, sine oculis; *y*, yellow.

Goldstein, 1990) is a minus-end directed kinesin motor protein (McDonald et al., 1990; Walker et al., 1990) that, when mutant, causes the formation of abnormal meiotic spindles in oocytes (Wald, 1936; Kimble and Church, 1983; Hatsumi and Endow, 1992*b*; Matthies et al., 1996). The wild-type Ncd motor protein has been proposed to function in establishing poles for assembly of bipolar meiosis I spindles (Kimble and Church, 1983; Hatsumi and Endow, 1992*a*,*b*; Matthies et al., 1996), replacing centrosomes in the spindle. A role in establishing bipolarity during assembly of the meiosis I spindle is consistent with the effects of null mutants on chromosome segregation (Sturtevant, 1929; Lewis and Gencarella, 1952), the abnormal spindles that have been observed in oocytes of the claret nondisjunctional (ca^{nd}) null mutant, and the association of the Ncd motor with meiotic spindle fibers (Hatsumi and Endow, 1992*a*; Matthies et al., 1996).

Assembly of the meiosis I spindle in wild-type oocytes and oocytes of the ca^{nd} null mutant has been examined by injection of rhodamine-conjugated tubulin to visualize spindle microtubules (Matthies et al., 1996). The results indicate that Ncd is required for normal kinetics of spindle assembly, as well as stabilization of the meiosis I spindle after assembly. Spindles were followed in this study from nuclear envelope breakdown through meiosis I spindle assembly and arrest of the meiosis I spindle.

Despite the emerging information regarding anastral spindle assembly in oocytes of *Drosophila*, the events of meiosis that occur after release from arrest and during progression through the meiotic divisions have not been adequately described. The classical account by Sonnenblick (1950) begins well into oocyte activation, with the spindle perpendicular to the oocyte surface. Spindles in mature arrested oocytes, however, are positioned parallel to the cortex (Theurkauf and Hawley, 1992; White-Cooper et al., 1993; Matthies et al., 1996). This raises the questions of how the spindle becomes oriented vertical to the cortex and when this occurs. There also exists a gap in our knowledge of spindle dynamics during re-entry into the meiotic cell cycle and completion of the meiotic divisions, which have not been directly visualized because of their rapid occurrence. The role of the Ncd motor during the meiotic divisions is also not known, although both the meiosis I and II spindles have been reported to be abnormal in *ncd* mutant oocytes (Wald, 1936; Hatsumi and Endow, 1992*b*).

To provide further information about meiotic spindle dynamics and Ncd function in the spindle, we fused the Ncd motor to the green fluorescent protein (GFP) of the jellyfish, *Aequorea victoria* (Prasher et al., 1992; Chalfie et al., 1994). An initial report of Ncd–GFP in mitosis in early embryos, including the rescue of an *ncd* null mutant by one of the first *ncd–gfp* gene fusions, has been published elsewhere (Endow and Komma, 1996). Here we show that Ncd–GFP is spindle-associated during meiosis in oocytes, like wild-type Ncd. The binding of Ncd–GFP to spindle microtubules provides a highly effective method for visualizing the meiotic spindle in live oocytes, resulting in new information regarding spindle dynamics during re-entry into meiosis and completion of the meiotic divisions. A mutant form of Ncd fused to GFP shows loss of function but binds to oocyte meiotic spindles, permitting spindle dynamics and the genesis of abnormal spindles in the presence of a loss-of-function Ncd motor to be observed. The results provide evidence that the Ncd microtubule motor is required for spindle elongation and, unexpectedly, stability of spindle fibers during the meiotic divisions. The Ncd motor probably also functions in polar body formation after the meiotic divisions, which are needed to prevent continued spindle-associated divisions of the maternal chromosomes after the initial two divisions.

Materials and Methods

Drosophila Stocks

Drosophila mutants and balancer chromosomes used in this study are described in Lindsley and Zimm (1992). The classical *ncd* mutant allele (O'Tousa and Szauter, 1980) is designated ncd^2 by Lindsley and Zimm (1992). ncd^2 was obtained from J. Kennison (National Institutes of Health, Bethesda, MD) in 1985 and has been maintained in our stock collection. For the present studies, chromosome 3 proximal to ebony (*e*, 3-70.7) in the ncd^2 stock was replaced by recombination, and the X chromosome and chromosome 2 were replaced using balancer chromosomes to remove any modifiers that may have accumulated in the stock. The recloned *e* ncd^2 chromosome was used as a control in genetic tests of the ncd^2*–gfp** transgene.

Sequence Analysis of ncd^2

The ncd^2 mutant allele was sequenced using as template DNA fragments amplified by PCR from genomic DNA of ncd^2 adult *Drosophila*, and cloned into pBluescript KS(+) (Stratagene, La Jolla, CA). The overlapping DNA fragments spanned the length of the ncd^2 coding region, starting upstream of the first in-frame AUG and continuing past the UAA stop codon (Endow et al., 1990) and included the two introns present in the *ncd* coding region. Changes in the DNA sequence that resulted in amino acid changes relative to wild-type Ncd were confirmed by sequence analysis of both DNA strands of two independent PCR clones.

Construction of ncd–gfp Plasmids

An *ncd–gfp* gene fusion was constructed in the P element vector, *pCaSpeR3* (Pirrotta, 1988; Thummel et al., 1988), by insertion into BglII plus EcoRI-digested plasmid of a 3.1-kb BamHI–EcoRI fragment containing the promoter and 5′ region of *ncd* (Yamamoto et al., 1989), and a 2.1-kb EcoRI cDNA fragment encoding the remainder of Ncd (Endow et al., 1990). The XbaI site in the plasmid at the 5′ end of the insertion was removed by digestion with NotI and StuI, followed by repair and religation. The plasmid was then digested with BamHI and XbaI, and the 3′ end of the *ncd* gene in the plasmid was replaced with a BamHI–AflII *ncd* fragment and an AflII–XbaI *gfp* fragment. The *ncd* fragment was synthesized by PCR using an *ncd* cDNA plasmid as template and the primers, 5′ ACA ATG GAC GGA GTG 3′ and 5′ TCA TCT TAA GGA AAT TGC CG 3′, followed by digestion with BamHI and AflII, and gel purification. The *gfp* fragment was synthesized by PCR using a *gfp–exu* plasmid (Wang and Hazelrigg, 1994) as template and the primers, 5′ GTG CTT AAG ATG AGT AAA GGA GAA 3′ and 5′ C CTT CTA GAA TTC TTT GTA TAG TTC 3′, followed by digestion with AflII and XbaI, and gel purification. The *ncd* PCR insertion in the recombinant plasmid and all but the last 50 bp of the *gfp* insertion were sequenced to confirm the absence of PCR synthesis errors. The plasmid, *pCaSpeR/ncd–gfp*, consists of a wild-type *ncd* cDNA fused in-frame to wild-type *gfp* and encodes residues 1–700 of Ncd (Endow et al., 1990) followed by residues 1–238 of GFP (Prasher et al., 1992), with a change of $D_{699} \rightarrow L$ in Ncd. Transcription of *ncd–gfp* is under the regulation of the *ncd* promoter.

A plasmid encoding wild-type Ncd fused to the $S_{65} \rightarrow T$ mutant GFP (Heim et al., 1995), denoted GFP*, was constructed by replacing the AflII–XbaI *gfp* fragment in *pCaSpeR/ncd–gfp* with an AflII–XbaI PCR fragment encoding the mutant *gfp*. The $S_{65} \rightarrow T$ mutation in the *pCaSpeR/ncd–gfp** plasmid was confirmed by DNA sequence analysis.

A plasmid containing *ncd* with the $G_{446} \rightarrow R$ mutation of the classical ncd^2 mutant allele fused to the $S_{65} \rightarrow T$ mutant *gfp*, ncd^2*–gfp**, was constructed by replacing the SphI–BamHI fragment of *pCaSpeR/ncd–gfp**

with an SphI–BamHI fragment encoding the $G_{446} \rightarrow R$ mutation. The SphI–BamHI fragment of the new plasmid, *pCaSpeR/ncd²–gfp**, was sequenced to confirm the presence of the $G_{446} \rightarrow R$ mutation and the absence of PCR synthesis mutations.

Germline Transformation and Genetic Tests for Null Mutant Rescue

For P element-mediated germline transformation, the *pCaSpeR/ncd–gfp*, *pCaSpeR/ncd–gfp**, and *pCaSpeR/ncd²–gfp** plasmids were injected into embryos of w^{1118} females crossed to *y w; Δ2-3 Sb/TM6 Ubx* males. Transformant lines were established and made homozygous in ca^{nd} null mutant females for cytological analysis of live or fixed oocytes and embryos. Females from the lines were tested genetically for rescue of ca^{nd}.

Tests of transgenes for rescue of ca^{nd} and tests of ncd^2 mutant effects on embryo viability and X chromosome segregation were carried out as described previously (Komma et al., 1991; Endow et al., 1994). Parental females were mated to tester $+/B^SYy^+$ or $y^2\ w^{bf}/B^SY$ males. Regular offspring of these matings are + females and B^S males. Meiotic nondisjunction of the X chromosome in oocytes results in B^S (X/X/Y) females and X/0 males; meiotic loss of the X results in X/0 males. Mitotic loss of the X in early embryos gives rise to gynandromorphs (X/X:X/0 mosaics). Minute offspring, haploid for chromosome 4, were scored but are excluded from calculations of total chromosome missegregation because of their highly variable recovery (Lindsley and Zimm, 1992). Calculations of meiotic nondisjunction and chromosome loss were performed as described (Komma et al., 1991; Endow et al., 1994). Statistical tests of significance were carried out using standard χ^2 and Poisson distribution tests, assuming the null hypothesis that the offspring being compared were from the same population (Komma et al., 1991).

Localization of Transgene Insertions

The cytological sites of transgene insertion were determined by in situ hybridization using a biotin-11-dUTP–labeled *ncd* cDNA probe, as described (Yamamoto et al., 1989). The *F24M1* and *F24M3 ncd–gfp* insertions were localized to 44B,C on 2R and 2A1,2 on the X chromosome, respectively. Recombination analysis of sine oculis (*so*, 2-57.1, 43B1-2) and bloated (*blo*, 2-58.5, 44F1-2 to 45E1-2) with *F24M1,* and yellow (*y*, 1-0.0, 1B1) and scute (*sc*, 1-0.0, 1B3) with *F24M3* was carried out to confirm the cytological map positions. The *ncd–gfp** transgene insertions, *M3M1* and *M9F1*, were localized by in situ hybridization to 42A,B at the base of 2R and 75C,D on 3L, respectively. The map positions were confirmed by recombination analysis of *so* and *blo* with *M3M1* and blistery (*by*, 3-48.7, 85D11-E3) with *M9M1*.

Visualization of GFP in Live Oocytes

Nonactivated live mature stage 14 oocytes were dissected from ovaries of *ncd–gfp*, *ncd–gfp**, or *ncd²–gfp** females immersed in a pool of light halocarbon oil (halocarbon oil 27; Sigma Chemical Co., St. Louis, MO) and transferred to a drop of light halocarbon oil on a slide (Theurkauf, 1994). Oocytes were positioned dorsal side up, and a coverslip fragment was mounted over the oocytes onto two layers of double-stick tape placed on either side to form a channel. Initial observations were carried out using a fluorescence microscope (Leitz Dialux 22; Leica, Inc., Rockleigh, NJ) equipped with a standard FITC or custom GFP (HQ470/40 excitation, Q495LP dichroic, HQ525/50BP emission; Chroma Technology Corp.) filter set.

For confocal microscopy, slides were prepared and oocytes were located under white light before laser scanning. Time lapse confocal images were collected through the oocyte chorion using a laser scanning confocal detector (MRC 600; BioRad, Richmond, CA) mounted on a microscope (Axiophot; Zeiss, Inc., Thornwood, NY) and equipped with a krypton/argon laser. The BioRad BHS or GR2 filter set (used with the T3 trichroic filter block; BioRad) or a custom confocal GFP filter set (Chroma Technology Corp., Brattleboro, VT; Endow and Komma, 1996) was used to image GFP. The custom GFP filter set increased the GFP signal over that collected with the BHS or GR2 sets by ~1.3 and ~1.8 times, respectively. The bandpass emission filter in the custom GFP and GR2 sets suppresses autofluorescence of the chorion and vitelline membrane when imaging GFP (Endow and Piston, 1997), improving image quality. A 10% neutral density filter was used for imaging Ncd–GFP and a 1% filter for Ncd–GFP*. The 488-nm line of the laser and an objective (63×/1.4 NA Planapochromat; Zeiss, Inc.) were used for image collection. Images were collected into stacks of 60 at 16.5 s intervals using the time lapse feature of COMOS software (BioRad) and 3 Kalman-averaged slow scans per image.

For activated live oocytes, mature stage 14 oocytes were dissected from ovaries of *ncd–gfp*, *ncd–gfp**, or *ncd²–gfp** females into *Drosophila* PBS (Robb, 1969) and transferred to a drop of light halocarbon oil on a glass slide. The chorion was partially removed under oil by pulling on the dorsal appendages with fine-tipped watchmaker's forceps, and a coverslip fragment was mounted over the oocytes, as described above for nonactivated oocytes. In some cases the halocarbon oil was bubbled briefly with O_2 before use. The meiotic spindles of activated live oocytes could be effectively visualized without removal of the chorion, although sharper images were usually obtained by removing the chorion over the spindle. Laser scanning confocal microscopy was carried out using the 488-nm line of the laser, the GR2 or custom GFP filter block, and a neutral density filter that transmitted 1 or 3% of the laser light. Images were collected into stacks at 16.5 or 23 s intervals with 3 or 5 Kalman-averaged slow scans for each image.

Analysis of Time Lapse Images

Stack files of time lapse images were opened, converted to single images, and saved as PICT or TIFF files using the public domain program, NIH Image v 1.59. Image contrast and size was adjusted as necessary using Adobe Photoshop v 3.0.4. Measurements of spindle length were carried out with NIH Image calibrated with a 10 μm bar superimposed on the images using COMOS (BioRad). The montages shown in Figs. 6 and 7 were made using the Crop and Make Montage stack macros of NIH Image. Image stacks were animated using NIH Image and recorded to videotape using NIH Image or Adobe Premiere v 4.0. Methods for making videotape recordings and QuickTime movies from GFP time lapse images are described in detail elsewhere (Endow and Piston, 1997). Video sequences of the figures can be viewed at http://abacus.mc.duke.edu

Indirect Immunofluorescence Labeling of Fixed Oocytes and Embryos

Nonactivated fixed oocytes were prepared by dissecting ovaries from wild-type (Oregon R), *ncd–gfp**, or *ncd²–gfp** females, partially submerged in modified Robb's medium (Theurkauf and Hawley, 1992) containing 4.7% (vol/vol) formaldehyde. Mature oocytes were teased from the ovaries, fixed for a total of 1.5 min at room temperature in the formaldehyde/saline solution, and then transferred into PBS. The chorion and vitelline membranes were removed from the fixed oocytes manually using fine-tipped watchmaker's forceps. Fixed oocytes were then incubated overnight at room temperature in TBST (TBS plus 0.3% Triton X-100; Williams et al., 1992) before blocking in TBST plus 10% fetal calf serum for 1–2 h. Oocytes were incubated in rhodamine-conjugated anti–α-tubulin monoclonal antibody (a gift of W. Sullivan; University of California, Santa Cruz, CA), as described (Endow et al., 1994). 5 μg/ml of DAPI (Boehringer Mannheim Corp., Indianapolis, IN) was added to one of the washes after antibody incubation to stain the chromosomes.

Normally activated fixed eggs at various stages of the meiotic divisions were obtained by collecting embryos at 12–15-min intervals from wild-type females or *ncd²–gfp** mutant females, followed by dechorionation, removal of the vitelline membrane, and fixation in MeOH/EGTA without taxol, as described previously (Hatsumi and Endow, 1992*b*). Some collections of wild-type or *ncd²–gfp** eggs were dechorionated manually before removal of the vitelline membrane rather than by treatment with Clorox, to save time. Rehydration of embryos, antibody staining, and subsequent washes were performed as previously described (Hatsumi and Endow, 1992*b*), except that TBST (TBS plus 0.1% Triton X-100) was used throughout instead of PBST (PBS plus 0.05% Triton X-100).

Antibody-stained oocytes and embryos were mounted in anti-fade solution consisting of 90% glycerol plus 0.1 vol of 10 mg/ml *p*-phenylenediamine in PBS, pH 9 (Stearns et al., 1991) for visualization of fluorescence.

Laser Scanning Confocal and Fluorescence Microscopy

Laser scanning confocal microscopy of fixed oocytes and embryos stained with rhodamine-conjugated anti–α-tubulin antibody was carried out using a scanning confocal detector (MRC 600; BioRad) equipped with a krypton/argon laser and attached to a microscope (Axiophot; Zeiss, Inc.). A 63X/1.4 NA Planapochromat objective and COMOS software (BioRad) were used to collect images of rhodamine-labeled spindles. Images of DAPI-stained chromosomes were collected using a cooled CCD camera (Pen-

taMax-1317-K; Princeton Instruments, Trenton, NJ) interfaced to a Power Macintosh 8100/100 PC and mounted on a fluorescence microscope (Dialux 22; Leica Inc., Deerfield, IL) with an Hg light source. A 63X/1.4 NA Planapochromat objective and IPLab Spectrum software (Signal Analytics Corp., Vienna, VA) were used for image collection.

Confocal or CCD camera images taken at several planes of focus were merged into single files using Adobe Photoshop v 3.0.4 to display the entire meiotic spindle or set of meiotic chromosomes in a single image. The CCD camera DAPI images were adjusted to the same size as the confocal spindle images by comparing confocal and CCD camera spindle images to one another. The DAPI images were then superimposed onto the confocal spindle images so that the relative positions of the chromosomes with respect to the spindles could be determined. These composite confocal plus CCD camera images were almost identical to merged CCD camera spindle and chromosome images, except that the confocal spindle images showed less out-of-focus detail.

Results

ncd–gfp Transgenes

A plasmid encoding an Ncd–GFP fusion protein was constructed by fusing a wild-type *ncd* cDNA in-frame to wild-type *gfp*. The *ncd–gfp* gene fusion is regulated by the native *ncd* promoter (Yamamoto et al., 1989) and encodes full-length Ncd (amino acids 1–700) followed by full-length GFP (residues 701–938). Amino acid 699 of Ncd was changed from aspartic acid to leucine during construction of the gene fusion. The GFP is at the COOH terminus of Ncd, adjacent to the motor domain, which contains ATP- and microtubule-binding sites that are required for motor function. Two introns that are present in the coding region of wild-type *ncd* were deleted in the *ncd–gfp* construct. An *ncd* cDNA transgene without the two introns was tested previously and shown to fully rescue the chromosome missegregation of the *ncd* null mutant, ca^{nd}, when present in one copy (Komma, D.J., and S.A. Endow, unpublished observation) or two copies (Endow et al., 1994). ca^{nd}, originally isolated after X irradiation (Lewis and Gencarella, 1952), contains a deletion of the *ncd* promoter and 5′ end of the *ncd* mRNA coding region and does not produce detectable *ncd* RNA transcripts (Yamamoto et al., 1989). Rescue of ca^{nd} by the *ncd* cDNA transgene indicates that the two introns present in the *ncd* gene are not required for normal expression of *ncd*.

Transformants with single insertions of *ncd–gfp* were recovered, and the *ncd–gfp* transgenes were transferred into *Drosophila* carrying ca^{nd}. The two *ncd–gfp* transgene insertions reported here, *F24M1* and *F24M3*, were mapped by in situ hybridization to 44B,C and 2A1,2, respectively, on chromosome 2R and the tip of the X chromosome. The cytological map positions were confirmed by recombination analysis of *so* and *blo* with *F24M1* and *y* and scute with *F24M3*.

Tests of function showed almost complete rescue of ca^{nd} for meiotic and mitotic chromosome segregation by two copies of the *ncd–gfp F24M1* transgene, resulting in a frequency of 0.004 X chromosome missegregation compared to 0.294 for ca^{nd} and <0.001 for wild type (Table I). Embryo viability (0.617) was partially rescued compared to 0.113 for ca^{nd} and 0.944 for wild type. Two copies of the *F24M3* transgene partially rescued ca^{nd} both for chromosome segregation and embryo viability (Table I). The incomplete rescue of ca^{nd} by *F24M1* and *F24M3* indicates a position effect on *ncd–gfp* expression or interference by GFP with Ncd function. *Drosophila* with four copies of the *ncd–gfp* transgene (two copies each of *F24M1* and *F24M3*) were also tested for rescue of ca^{nd}. These females showed no significant differences from wild type with respect to chromosome segregation (0.002 missegregation compared with <0.001 for wild type; $P = 0.06$) or embryo viability (0.933 compared with 0.944 for wild type; $\chi^2 = 1.79$, 1 degree of freedom, $0.5 > P > 0.1$; Table I). The results demonstrate that the *ncd–gfp F24M1* and *F24M3* insertions together can rescue ca^{nd} and replace the function of the wild-type Ncd microtubule motor protein.

Drosophila carrying the *ncd–gfp** transgene, with wild-type *gfp* replaced by the $S_{65} \rightarrow T$ mutant *gfp* (Heim et al., 1995), were also recovered. The *ncd–gfp** transgenes, *M3M1* and *M9F1*, were localized by in situ hybridization to 42A,B at the base of 2R and 75C,D on 3L, respectively. The cytological map positions were confirmed by recombination analysis of *so* and *blo* with *M3M1* and blistery with M9F1. Tests of homozygous *M3M1* or *M9F1* showed partial rescue of ca^{nd}, while four copies of *ncd–gfp**, two each of *M3M1* and *M9F1*, showed essentially complete rescue of ca^{nd} both for chromosome segregation and embryo viability (Endow and Komma, 1996).

Association of Ncd–GFP with Oocyte Meiotic Spindles

Initial observations using a cooled CCD camera or laser scanning confocal microscopy to visualize GFP fluorescence in live *ncd–gfp* oocytes revealed green fluorescent spindles, demonstrating that the *ncd–gfp* transgene is ex-

Table I. Rescue of the ca^{nd} Null Mutant by the ncd–gfp Transgene

Female parent	Copies of ncd^+	Total gametes	Gametic		Zygotic X loss	Total* adults	Total embryos	Total missegregation	Embryo viability
			X nd	X loss					
1. ca^{nd}/ca^{nd}	0	143	0.238	<0.007	0.056	144	1,277	0.294	0.113
2. *F24M1/F24M1;* ca^{nd}/ca^{nd}	2	1,515	<0.001	0.003	0.001	1,513	2,454	0.004	0.617
3. *F24M3/F24M3;* ca^{nd}/ca^{nd}	2	664	0.012	0.021	0.011	670	1,217	0.044	0.551
4. *F24M3/F24M3; F24M1/F24M1;*ca^{nd}/ca^{nd}	4	1,767	0.002	<0.001	<0.001	1,765	1,891	0.002	0.933
5. +/+	2	1,883	<0.001	<0.001	<0.001	1,883	1,995	<0.001	0.944

Females of the indicated genotypes were tested for embryo viability and segregation of the X chromosome. Females carrying the *ncd–gfp F24M1* or *F24M3* transgene were y^2 w^{bf}. Wild-type (+/+) females were Oregon R. Total missegregation is that of the X chromosome. Data for ca^{nd} were for a newly cloned stock of ca^{nd} in which the X chromosome and chromosome 2 had been replaced to remove any modifiers that had accumulated in the stock; the data were taken from Endow and Komma (1996).
*Including M offspring.
nd, meiotic nondisjunction; *M*, minute.

pressed and can be detected in live oocytes. The spindle fluorescence indicated that the Ncd–GFP fusion protein is associated with the oocyte meiotic spindle, as observed previously for wild-type Ncd using antibody staining (Hatsumi and Endow, 1992*a*; Matthies et al., 1996). Association of Ncd–GFP with meiotic spindles permits analysis of meiotic spindle dynamics in live oocytes of *Drosophila.*

Live *ncd–gfp* oocytes were prepared for observation by dissection from ovaries either under halocarbon oil or into *Drosophila* PBS (Robb, 1969), followed by mounting under oil. Oocytes dissected under oil were interpreted to be nonactivated, by comparison with nonactivated fixed oocytes prepared by dissecting ovaries directly into fixative. Oocytes dissected into *Drosophila* PBS showed dramatic changes in the spindle, including meiosis I spindle elongation and assembly of tandem meiosis II spindles. These oocytes are interpreted to be activated since the cytological changes in the spindle are consistent with oocyte activation, as evidenced by analysis of normally activated fixed eggs. These results are described below.

Meiotic Spindle Dynamics in Nonactivated Live Oocytes

Spindles of nonactivated live *ncd–gfp* oocytes, prepared by dissection from ovaries of females under halocarbon oil, could be observed through the chorion by laser scanning confocal microscopy. The tapered bipolar spindles, located near the base of the dorsal appendages, were brightly fluorescent with Ncd–GFP (Fig. 1). The dark region in the center of the fluorescent spindles was presumed to correspond to the chromosomes, which exclude Ncd–GFP. This was confirmed by antibody staining of nonactivated fixed oocytes. Spindles of nonactivated live oocytes imaged without removal of the chorion were relatively stable, remaining in the same position throughout the 15–30 min periods of image collection with little or no net change in length or orientation. The spindle shown in Fig. 1 was from a ca^{nd} oocyte with four copies of the *ncd–gfp** transgene. Stable metaphase I meiotic spindles were also observed in nonactivated live oocytes with one copy of the *ncd–gfp** transgene or four copies of the *ncd–gfp* transgene.

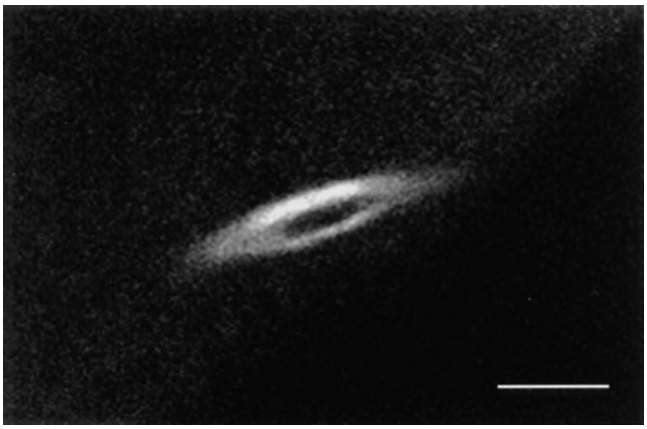

Figure 1. Meiosis I spindle in a nonactivated live *ncd–gfp** oocyte. The image was taken from a time lapse series of an *ncd–gfp** oocyte that was prepared by dissection under oil. The spindle was relatively stable, showing only slight changes in position and orientation during the 16.5-min observation time. Bar, 5 μm.

Despite their relatively stable positions, dynamic changes in the spindles of nonactivated live oocytes were occurring that could be detected over time. These changes comprised small lengthwise extensions and contractions of the spindles and alternating clockwise and counter clockwise rotational movements around their long axis, as diagrammed in Table II. These slight movements of the spindle were observed in all of the nonactivated live oocytes that were imaged (n = 13) and were best analyzed by animating the time lapse images and determining differences in orientation and position of the spindles over time. The spindles of most nonactivated live oocytes showed both extensions/contractions and rotational movements, but no net change in length or position over time (Table II). Spindles of several oocytes showed more extensive movements: one spindle rotated two to three revolutions around its long axis during the first 4 min of image collection before assuming a more stable position, and one spindle rotated approximately a quarter turn over the 16.5-min observation time. Another spindle moved lengthwise a quarter of its length and then returned to its original position, and one spindle elongated ~75% of its length. The oocyte containing this last spindle may have been unintentionally activated by the continuous laser irradiation. With the exception of this oocyte, none of the nonactivated live oocytes with intact chorions showed changes in the spindle that resembled completion of meiosis I and progression into meiosis II. These oocytes were therefore interpreted as arrested in meiosis I.

The spindles of nonactivated live oocytes were typically observed through the chorion. Removal of the chorion from the live oocytes resulted in changes that included elongation of the spindle followed by the formation of two tandem meiosis II spindles. These changes are consistent with oocyte activation and occurred even though the oocytes were dissected under oil and the chorion was removed under oil. These changes were observed in 3/3 oocytes that were prepared in this manner and observed. Perturbation of nonhydrated *Drosophila* oocytes can therefore cause oocyte activation, resulting in re-entry into meiosis and completion of the meiotic divisions.

Table II. Spindle Movement in Nonactivated Live Oocytes

No net change over time			Net change	
Extension/ contraction	Alternating CW and CCW rotations	Lengthwise movement	Elongation	Rotation
				
12	7	1	1	1 (2–3 revolutions) 1 (1/4 turn)

Spindle movements are shown of nonactivated live oocytes (n = 13) that were prepared under oil and imaged for 15–30 min. The schematic diagrams illustrate the types of movement that were detected. The oocyte in which the spindle underwent a net elongation may have been unintentionally activated by the continuous laser irradiation. The spindle movements of the other oocytes did not resemble resumed meiotic divisions.

*Barely detectable rotational movement.

CW, clockwise; *CCW*, counter clockwise.

Chromosomes associated with the meiotic spindles could not be visualized in nonactivated live *ncd–gfp* oocytes in the absence of further perturbating treatments, such as injection of fluorescent DNA dyes, that could cause oocyte activation. Nonactivated fixed *ncd–gfp* and wild-type oocytes were therefore prepared and stained with anti–α-tubulin antibody and DAPI for comparison with spindle images from nonactivated live *ncd–gfp* oocytes and determination of the chromosome configurations. Metaphase I–arrested spindles in nonactivated fixed wild-type oocytes, merged with DAPI-stained chromosomes, are shown in Fig. 2. The fluorescent spindles visualized by tubulin antibody staining are similar in appearance to the Ncd–GFP fluorescent spindles. The highly condensed metaphase I chromosomes are present in the center of the spindle, in a position corresponding to the dark regions in the spindles visualized with Ncd–GFP. The spindles stained with anti-tubulin antibody also showed a dark region in the center corresponding to the chromosomes. The small dotlike chromosome 4 could be observed either associated with the remainder of the chromosomes and identified as a small protrusion at the ends of the chromosome mass (Fig. 2 *A*, *arrows*), or separated from the rest of the chromosomes and positioned closer to the poles (Fig. 2 *B*, *arrows*). The spindle and chromosome configurations of nonactivated fixed *ncd–gfp* oocytes, prepared using the same methods as nonactivated fixed wild-type oocytes and stained with anti-tubulin antibody and DAPI, were similar in appearance to the spindles and chromosomes shown in Fig. 2.

Rotation of the Meiotic Spindle in Activated Live Oocytes

Oocytes were also prepared by dissection from ovaries of *ncd–gfp* or *ncd–gfp** females into *Drosophila* PBS (Robb, 1969). Mature oocytes, visibly swollen by the brief (<3 min) immersion in the undiluted saline solution, were transferred to a drop of halocarbon oil on a slide, the chorion was removed from the anterior of the oocyte, and a coverslip was mounted over the oocytes. Time lapse images collected for periods of 15–50 min by laser scanning confocal microscopy showed that the meiotic spindles of live oocytes prepared by immersion in *Drosophila* PBS exist in a highly dynamic state. As an example, the spindle shown in Fig. 3 was first observed parallel to the oocyte surface (Fig. 3 *A*). The spindle elongated (Fig. 3 *B*), contracted, and then underwent an acute pivoting movement (Fig. 3 *C*) that reoriented the spindle from its initial position parallel to the oocyte surface into a position perpendicular to the oocyte cortex (Fig. 3 *D*). Fig. 3 *D* shows an image looking down the long axis of the spindle formed by the spindle poles, with the dark "holes" corresponding to the chromosomes, based on fixed oocytes and embryos stained for tubulin and DNA. The spindle remained in this position for at least 9.2 min, rotating around its long axis.

Rotations of the spindle around its long axis, after pivoting vertical to the cortex, were either clockwise or counter clockwise, or rapidly alternating clockwise and counter clockwise rotations. Spindles of 11 oocytes were analyzed after pivoting. Six spindles showed only rapidly alternating rotations, three rotated clockwise accompanied by rapidly alternating rotations, one only rotated clockwise, and two rotated counter clockwise and also showed rapidly alternating rotations.

Spindles of oocytes prepared by immersion in *Drosophila* PBS could rotate around their long axis before or after pivoting vertical to the oocyte surface, and several spindles elongated or contracted, as shown in Fig. 3. Microtubules, either single fibers or bundles, could be seen in images in which the spindles were cross-sectioned, projecting out from the spindles. Comparison of successive images in the time lapse sequences gave the impression that rapid shortening and elongation of the spindle microtubules was occurring and that the spindle was in a highly dynamic state.

Meiosis I to II Progression in Activated Live Oocytes

Spindles of oocytes that were prepared by immersion in *Drosophila* PBS could spontaneously complete the meiosis I and II divisions, permitting, for the first time, visualization of spindle dynamics during the transition from meiosis I to II. The meiosis I spindle shown in Fig. 4 *A* was

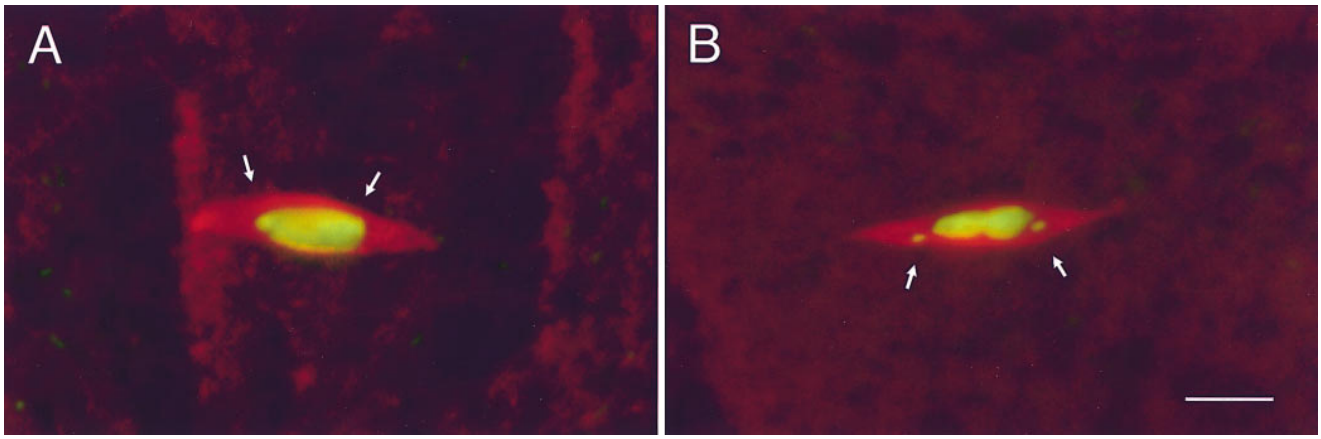

Figure 2. Metaphase I spindles in nonactivated fixed wild-type oocytes. Fixed oocytes were stained with anti–α-tubulin antibody (*red*) and DAPI (*green*) to visualize meiotic spindles and chromosomes. The position of the chromosomes in the spindle corresponds to the dark hollow in the center of the spindle in the live *ncd–gfp** oocyte (Fig. 1). The dot-like fourth chromosomes (*arrows*) were found either (*A*) associated with the condensed mass of chromosomes or (*B*) positioned closer to the poles in the metaphase I spindles. Bar, 5 μm.

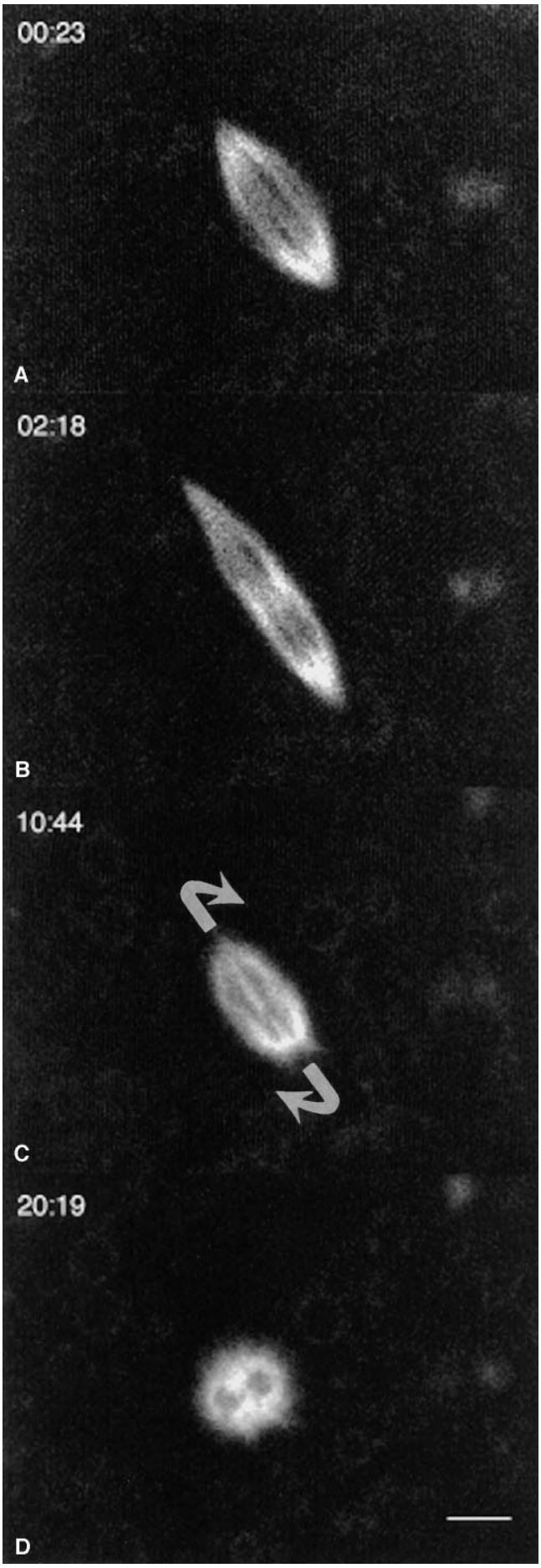

positioned obliquely to the oocyte surface and was viewed from an angle that allowed imaging of the entire spindle. The spindle extended into an elongated, tapered meiosis I spindle (Fig. 4 *B*), measuring ~30 μm from pole to pole, and then rapidly reassembled into two tandemly arrayed meiosis II spindles (Fig. 4, *C* and *D*). Assembly of the tandem meiosis II spindles occurred by the formation of a bright focus of Ncd–GFP in the center of the elongated meiosis I spindle (Fig. 4 *B*, *arrow*), followed by the establishment of two central spindle poles. The tandem meiosis II spindles were interpreted to assemble by rapid sliding of the spindle microtubules against one another, based on the movements of the spindle observed in the time lapse sequence. The transition into meiosis II occurred without disassembly of the meiosis I spindle and involved reorganization of the spindle fibers into the two tandem meiosis II spindles.

The time required to complete the meiotic divisions was determined by analysis of oocytes for which a complete sequence of meiosis I and II had been recorded. Meiosis I and II in time lapse sequences of three oocytes with four copies of the *ncd–gfp* transgene each lasted ~2.5–5 min, giving an estimate of ~5–10 min for completion of both divisions. In a previous study by other workers, eggs were collected for 5 min and fixed after an additional 5 min for a total development time of 5–10 min, and then stained and analyzed (Riparbelli and Callaini, 1996). 37% of the eggs were in meiosis I, 51% were in meiosis II, and 12% were in mitosis. This distribution is consistent with our estimate of ~5–10 min for completion of both meiotic divisions.

To determine if the spindles observed in activated live *ncd–gfp* oocytes resembled those of normally activated eggs, wild-type embryos collected at 0 to 12–15-min intervals were fixed and stained with anti-tubulin antibody and DAPI. The meiosis II spindles of normally activated fixed eggs were typically perpendicular to the cortex and aligned in tandem (Fig. 5). A faint ring-like central spindle pole body consisting of foci of tubulin with radiating microtubules could be observed between the two meiosis II spindles (Fig. 5 *A*, *arrow*). Other spindles showed only diffuse tubulin staining in the region between the two meiosis II spindles (Fig. 5 *B*). The central pole body of meiosis II spindles of normally activated fixed eggs was also stained by anti-Ncd antibody (not shown).

A Loss-of-function ncd Mutant and ncd–gfp Transgene

ncd^2 is a classical mutant of *ncd* that was originally isolated after EMS mutagenesis. The mutant was shown to fail to complement *ca*nd for chromosome missegregation (O'Tousa and Szauter, 1980), but a large-scale genetic analysis of the effects of *ncd*^{2} has not been reported previously. Tests of *ncd*^{2} mutant females showed markedly reduced embryo vi-

Figure 3. Meiotic spindle dynamics in an activated live *ncd–gfp* oocyte. Images from a time lapse series showing, from top to bottom, the spindle initially positioned parallel to the surface of the oocyte (*A*) and elongation of the spindle (*B*), followed by contraction and pivoting (*C*) into a vertical position with respect to the oocyte surface (*D*). The spindle remained in this position at least 9.2 min after pivoting, rotating around its long axis. Time in minutes and seconds is shown on each image. Bar, 5 μm.

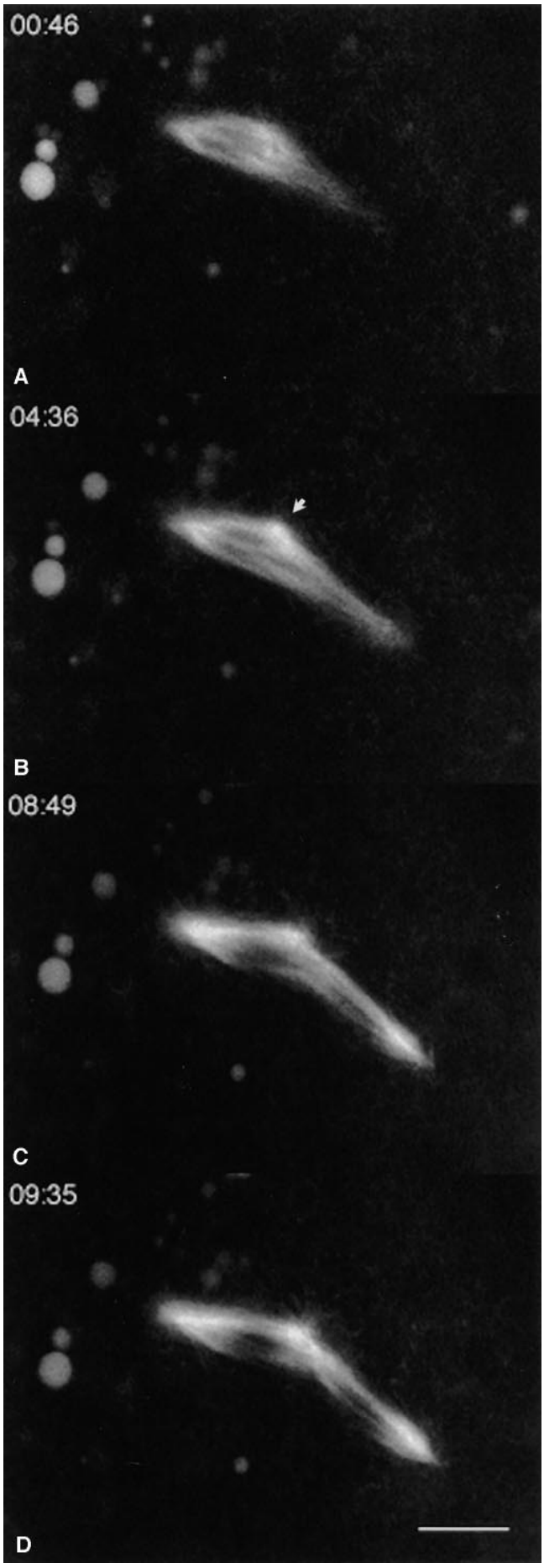

ability and elevated chromosome nondisjunction and loss compared to wild type (Table III). *ncd²* shows a slightly more severe effect on embryo viability (0.098) than *ca^nd* (0.113), but there is no significant difference in total X chromosome missegregation between *ncd²* and *ca^nd* (χ^2 = 0.371, 1 degree of freedom, $0.5 < P < 0.9$). Chromosome missegregation is fully rescued in heterozygous *ncd²*/+ females, but embryo viability (0.810 compared to 0.944 for wild type) is only partially rescued (Table III). *ncd²* therefore behaves like a loss-of-function mutant of *ncd* with respect to chromosome segregation and shows a small semidominant effect on embryo viability. The mutant *ncd²* gene is transcribed (Yamamoto et al., 1989), and the mutant protein is spindle-associated (Hatsumi and Endow, 1992*a*). The cytological effects of *ncd²* on meiotic spindles were found previously to be the same as those of *ca^nd* (Hatsumi and Endow, 1992*b*).

Sequence analysis of the coding region of *ncd²* revealed four amino acid changes, $G_{446} \rightarrow R$, $A_{566} \rightarrow S$, $G_{696} \rightarrow A$, and $N_{697} \rightarrow S$, compared to wild-type Ncd. The $G_{446} \rightarrow R$ missense mutation affects a glycine residue in the ATP-binding motif of Ncd, IFAYGQTGSGKTYTMD**G**, that is highly conserved among the kinesin proteins. This amino acid change is the likely cause of the loss of function of *ncd²*. Of the other changes in *ncd²*, $A_{566} \rightarrow S$ is a conservative amino acid change, $G_{696} \rightarrow A$ lies outide the motor domain, and $N_{697} \rightarrow S$ is a polymorphism found in some presumed wild-type strains. No other nucleotide substitutions were found in *ncd²* that result in missense mutations, or changes in the introns or intron/exon boundaries compared to *ncd⁺*.

The $G_{446} \rightarrow R$ missense mutation, but not the other 3 amino acid changes in *ncd²*, was introduced into an *ncd–gfp** plasmid containing the $S_{65} \rightarrow T$ mutant *gfp*, and the plasmid was injected into embryos for germline transformation. Transformants carrying the *ncd²*–gfp* transgene were recovered, and the transgenes were made homozygous in *ca^nd* females. The *ncd²*–gfp* transgene that was analyzed in this study is designated *M4F1*. The *ncd²*–gfp* *ca^nd* females showed poor fertility, high egg inviability, and elevated chromosome missegregation that paralleled the effects of *ncd²* (Table III). The effects of the *M4F1 ncd²-gfp** transgene on chromosome segregation were not significantly different from those of *ncd²* (χ^2 = 0.944, 1 d.f., $0.5 < P < 0.9$), although *M4F1* showed a slightly more severe effect on embryo viability (0.085) than *ncd²* (0.098). Females carrying one copy of *M4F1* together with one *ncd⁺* allele (*M4F1*; *ca^nd*/+ females) showed complete rescue for chromosome segregation, but embryo viability (0.886 compared with 0.944 for wild type) was only par-

Figure 4. Meiosis I to meiosis II progression in an activated live *ncd–gfp* oocyte. Time lapse images showing, from top to bottom, the meiosis I *ncd–gfp* oocyte spindle (*A*), elongation of the meiosis I spindle (*B*), reassembly into two tandem meiosis II spindles, and progression into meiosis II (*C* and *D*). Time in minutes and seconds is shown on each image. The arrow (*B*) indicates a bright focus of Ncd–GFP where the central spindle poles form. The spindles are positioned obliquely to the oocyte cortex, permitting the meiosis I and II spindles to be completely imaged. The interior of the oocyte is to the left. Bar, 10 μm.

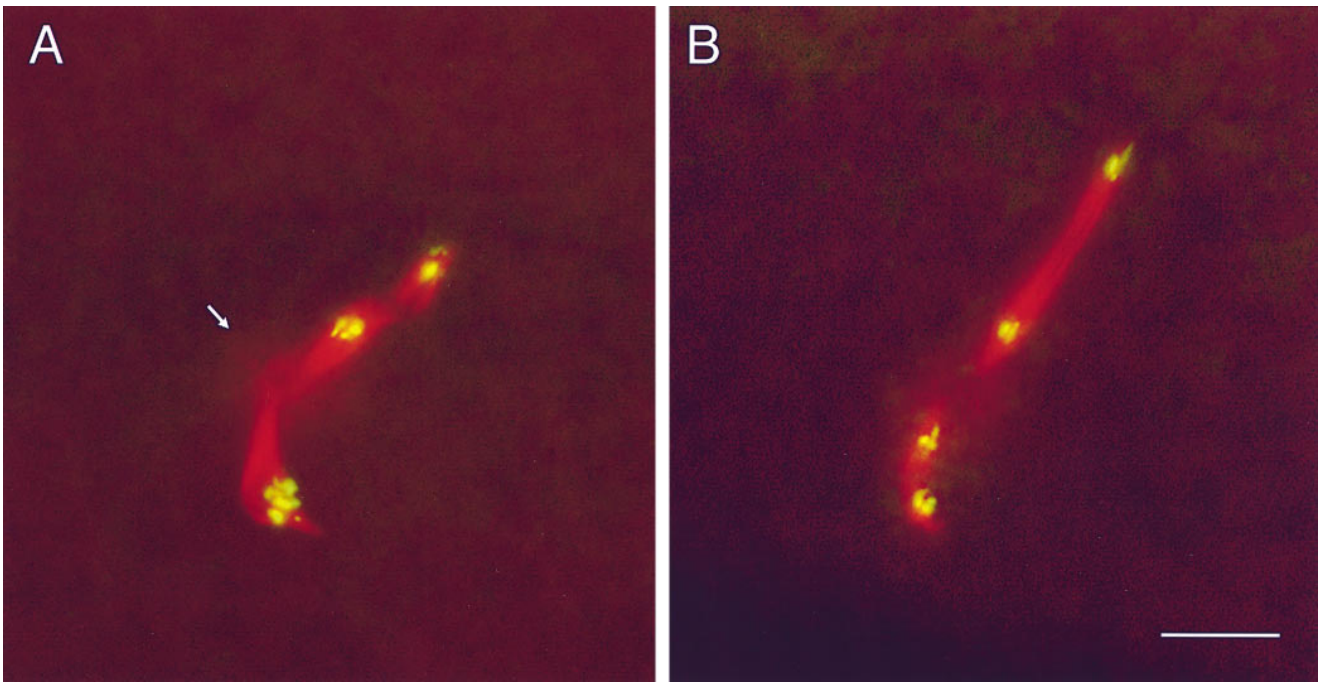

Figure 5. Meiosis II spindles in normally activated fixed wild-type eggs. Normally oviposited wild-type eggs were fixed and stained with anti–α-tubulin antibody (*red*) and DAPI (*green*) to visualize the spindles and chromosomes. The meiosis II spindles are perpendicular to the cortex and are viewed down their long axis. The bottom spindle in each image, which is closer to the surface of the embryo, is slightly delayed relative to the more internal spindle; this is probably an artifact caused by the time required for penetration of the fixative. (*A*) Meiosis II spindles in early (*bottom*) and mid- (*top*) anaphase. The faint central spindle pole body (*arrow*), which consists of foci of tubulin in a ring-like array with radiating microtubules, can be observed in the region between the two spindles. (*B*) Meiosis II spindles in mid- (*bottom*) and late (*top*) anaphase. The central spindle pole body appears as a diffuse array of microtubules between the two spindles. Bar, 10 μm.

tially rescued (Table III). The *M4F1 ncd²–gfp** transgene therefore closely parallels the *ncd²* mutant allele in its effects on chromosome segregation and embryo viability.

Meiotic Divisions in Loss-of-Function Mutant Oocytes

Green fluorescent spindles were not detected in nonactivated live *ncd²*–gfp* oocytes prepared by dissection under halocarbon oil and observed by laser scanning confocal microscopy. Nonactivated fixed oocytes stained with α-tubulin antibody and DAPI to visualize spindles and chromosomes contained unstained or faintly stained spindles, or partially formed abnormal spindles (not shown). Fully formed meiosis I spindles were not observed in the nonactivated fixed mutant oocytes (n = 104), even though mature oocytes were selected for the cytological analysis. The condensed meiotic chromosomes associated with the spindles also appeared to be at an earlier stage than chromosomes in nonactivated fixed wild-type mature oocytes. It is therefore probable that spindle assembly and maturation of the *ncd²–gfp** mutant oocytes is delayed relative to wild type.

Live *ncd²–gfp** oocytes, prepared by dissection into *Drosophila* PBS, contained green fluorescent spindles, provid-

Table III. The ncd²–gfp Transgene Fails to Rescue the ca^nd Null Mutant*

Female parent	Copies of *ncd²*	Total gametes	Gametic		Zygotic X loss	Total* adults	Total embryos	Total missegregation	Embryo viability
			X nd	X loss					
1. ca^{nd}/ca^{nd}	0	143	0.238	<0.007	0.056	144	1,277	0.294	0.113
2. $ca^{nd}/+$	0	1,569	0.003	<0.001	<0.001	1,567	1,748	0.003	0.896
3. ncd^2/ncd^2	2	79	0.101	0.127	0.127	155	1,582	0.355	0.098
4. $ncd^2/+$	1	1,829	<0.001	<0.001	<0.001	1,830	2,258	<0.001	0.810
5. *M4F1/M4F1*; ca^{nd}/ca^{nd}	2	86	<0.012	0.326	0.070	98	1,153	0.396	0.085
6. *M4F1;*$ca^{nd}/+$	1	3,322	<0.001	0.001	<0.001	3,321	3,747	0.001	0.886
7. +/+	0	1,883	<0.001	<0.001	<0.001	1,883	1,995	<0.001	0.944

Females carrying the *ncd²* mutant allele of *ncd* or the *ncd²–gfp*M4F1* transgene were tested for embryo viability and segregation of the X chromosome. Females carrying the *ncd²–gfp* M4F1* transgene were y^2 w^{bf}. Total missegregation is that of the X chromosome. The data shown for ncd^2/ncd^2 were obtained using a newly recloned *ncd²* allele. Data from Table I for ca^{nd} and + females are shown for comparison.

*Including M offspring.

nd, meiotic nondisjunction; *M*, minute.

ing evidence that the *ncd*^{2}*–gfp** transgene is expressed and the Ncd^2-GFP* protein is associated with meiotic spindles. The basis of the ability to visualize spindles in activated live oocytes but not nonactivated live oocytes is not certain, but is likely to be due to changes in the oocyte that occur upon activation. The spindles in the live mutant oocytes were activated to complete the meiotic divisions, but the divisions were highly abnormal. In the time lapse series shown in Fig. 6, a spindle was initially observed that appeared to be formed of closely apposed spindles (*A* and *B*). The spindle was interpreted to be in meiosis I, based on the subsequent events in the time lapse sequence. Multiple poles arose by separation of the spindles at the poles (Fig. 6 *C*, *arrows*). The spindles failed to extend into the highly elongated meiosis I spindles typical of wild-type oocytes. A small focus of Ncd^2–GFP* formed in part of the spindle (Fig. 6 *C*, *arrowhead*), marking the position of the meiosis II-like central spindle poles, but normal meiosis II spindles failed to form. Instead, a short multipolar spindle arose by movement of the newly formed central spindle poles away from the rest of the spindle, pulling on microtubules attached to the original poles (Fig. 6, *D–H*).

Although spindles in most of the activated live mutant oocytes failed to elongate into typical meiosis I spindles, spindles in 2 of the 23 mutant oocytes that were recorded did show elongation typical of wild-type meiosis I spindles. Elongation of spindles in these two oocytes was followed by the formation of two independent pairs of central spindle poles in the closely apposed spindles that comprised the spindle; movement of the new poles in opposite directions resulted in the formation of cruciform spindles.

Multiple spindles were present in some activated live mutant oocytes that arose by separation of meiotic spindles into several spindle-like components. As an example, the time lapse series in Fig. 7 shows three spindles that were separated from one another when initially observed. Movement of the spindles in different directions caused them to become somewhat more widely separated (Fig. 7, *A–C*). The spindle fibers in the centers of the spindles then began fragmenting (Fig. 7, *D–H*), releasing the poles from the spindles (*G* and *H*). Fluorescent particles, presumed to be microtubule fragments bound to Ncd^2–GFP*, were observed in the cytoplasm and formed a hazy network in the center of the spindles (Fig. 7, *E–H*). The released poles of the spindles moved far from the original site of the spindles and could be observed in the oocyte after the time lapse imaging, separated from one another by as much as 75–80 μm.

Progression of the meiotic divisions was slow in the activated live mutant oocytes compared with wild-type oocytes, requiring 30 min or longer for completion of two divisions, and spindles in some mutant oocytes continued dividing after the initial two divisions without undergoing disassembly.

Spindles in normally activated fixed mutant eggs were examined for comparison with spindles in activated live mutant oocytes. Mutant eggs in various stages of the meiotic divisions were collected at 0–15 min intervals, fixed,

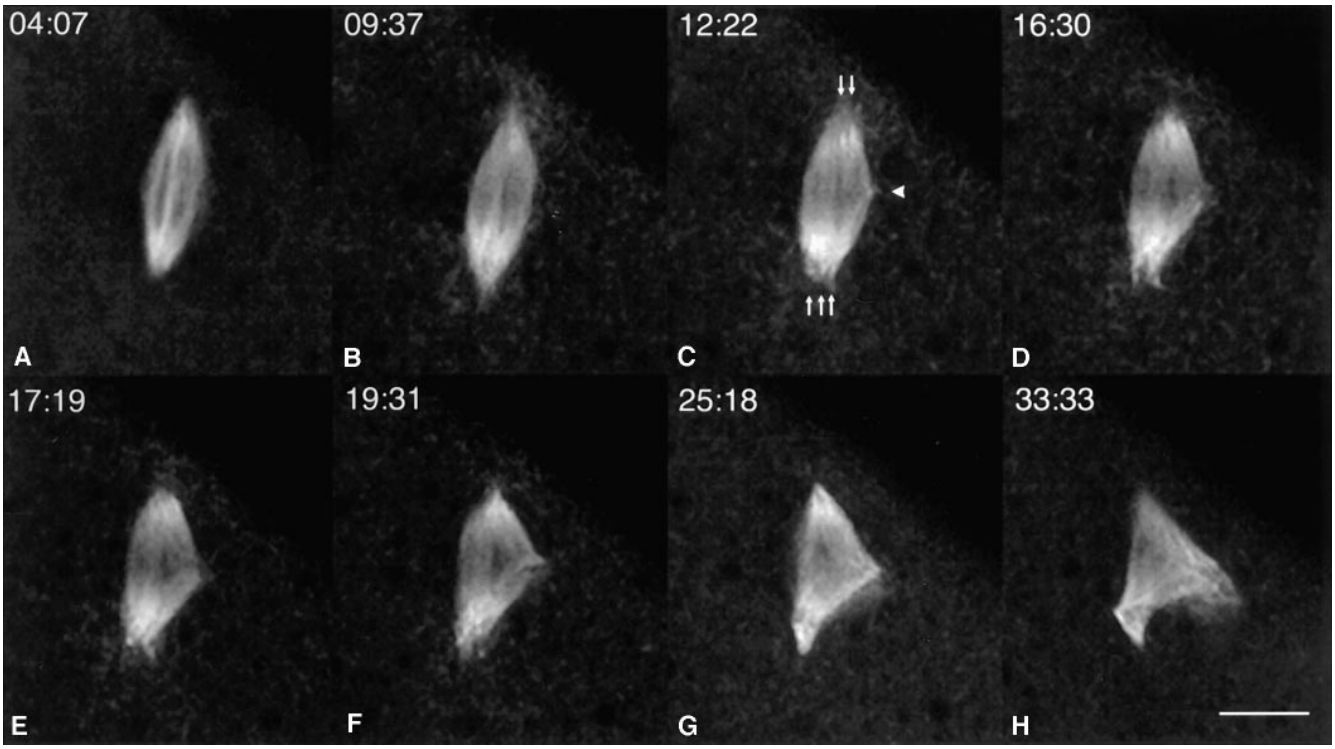

Figure 6. Meiotic divisions in an activated live *ncd*^{2}*–gfp** mutant oocyte. Images from a time lapse sequence of an activated live *ncd*^{2}*–gfp** mutant oocyte show, from left to right and top to bottom, the spindle consisting of closely apposed separate spindles (*A* and *B*), separation of the spindle poles (*C*, *arrows*), and the formation of a small focus of Ncd^2–GFP* (*C*, *arrowhead*) that marks the position of the central spindle poles. Movement of the new spindle poles away from the rest of the spindle (*D–H*) caused a short multipolar spindle to form (*H*) due to the attachment of the microtubules to the original poles. Time in minutes and seconds is indicated on each frame. Bar, 10 μm.

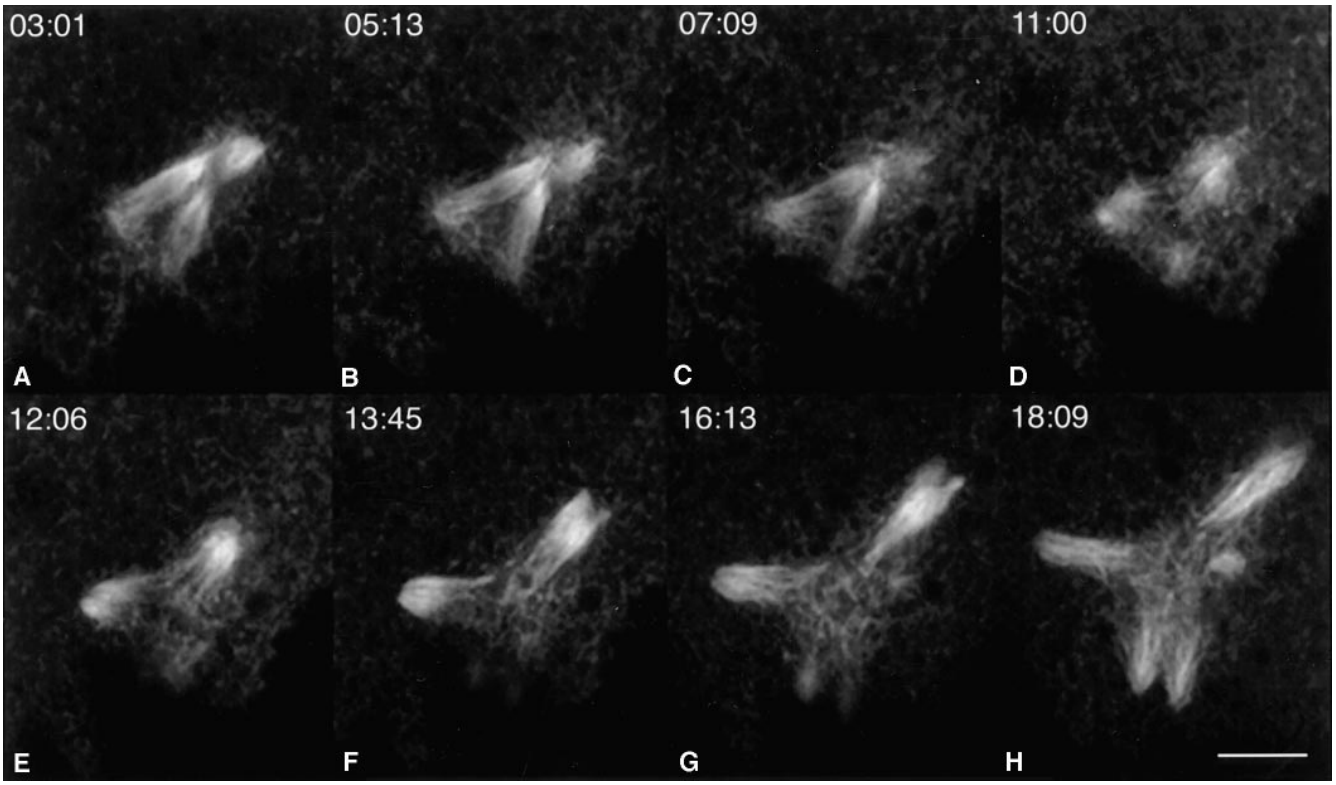

Figure 7. Release of spindle poles in an activated live *ncd*^{2}*–gfp** mutant oocyte. Time lapse images of an activated live *ncd*^{2}*–gfp** mutant oocyte show, from left to right and top to bottom, three spindles that were initially separated from one another moving in different directions to become somewhat more widely separated (*A–C*), fragmentation of spindle fibers in the centers of the spindles (*D–H*), and release of the spindle poles (*G* and *H*). Fluorescent particles are present in the cytoplasm and form a hazy network in the center of the spindles (*E–H*). These are probably microtubule fragments bound to Ncd^2–GFP*. Time in minutes and seconds is indicated on each frame. Bar, 10 μm.

and stained with α-tubulin antibody and DAPI to visualize the meiotic spindles and chromosomes. Anaphase I and metaphase II spindles in normally activated fixed *ncd*^{2}*–gfp** mutant eggs are shown in Fig. 8. Several of the normally activated fixed mutant eggs exhibited a haze of microtubules associated with the meiotic spindles (Fig. 8 *A*), as observed in activated live mutant oocytes. Multiple spindles were present, both in meiosis I and II, with each of the separated chromosomes, including the small chromosome 4 (Fig. 8 *A*, *arrows*), associated with a spindle spur or spindle. The spindles were oriented obliquely or vertically with respect to the embryo cortex. The arrow in Fig. 8 *B* indicates a cross-sectioned spindle that is vertical, associated with a spindle spur, indicating that the mutant Ncd–GFP does not prevent reorientation of the spindles perpendicular to the cortex. One or more of the spindle-associated meiotic chromosomes in some eggs was widely separated from the others. For example, one of the 8 half-bivalent chromosomes was missing from the cluster of spindle-associated metaphase II chromosomes in one egg. The missing chromosome was found 85–90 μm from the nearest chromosome in the cluster, associated with a small spindle remnant.

Normally activated fixed early eggs of *ncd*^{2}*–gfp** mutant females frequently contained multiple spindle-associated chromosomes that exceeded the 4N = 16 number expected upon completion of the two meiotic divisions. The spindles lacked centrosomes, like the oocyte meiotic spindles, and, in many eggs, were abnormal (either multipolar, branched, or spurred). The fixed mutant egg shown in Fig. 8 *C* contained 18 chromosomes or pairs of nondisjoined sister chromatids. Many of the chromosomes were separated from one another and associated with separate spindles, and some of the chromosomes showed anaphase configurations, as if they were in the process of dividing. One of these is indicated by an arrow. The spindles were located near the cortex of the egg, where the polar bodies are found in wild-type embryos. The egg was unfertilized, and no mitotic spindles were observed. The >4N chromosomes in this and other eggs probably arose by continued meiotic divisions of the maternal chromosomes. This interpretation is consistent with the more than two meiotic divisions that were observed in activated live mutant oocytes.

Discussion

GFP as a Fluorescent Tag to Monitor Meiotic Spindle Dynamics

The meiotic divisions in oocytes of most organisms, including *Drosophila*, have not been directly visualized previously. Several steps after oocyte activation occur very rapidly and have not been observed even in rapid collections of eggs analyzed by fixation and antibody staining. These

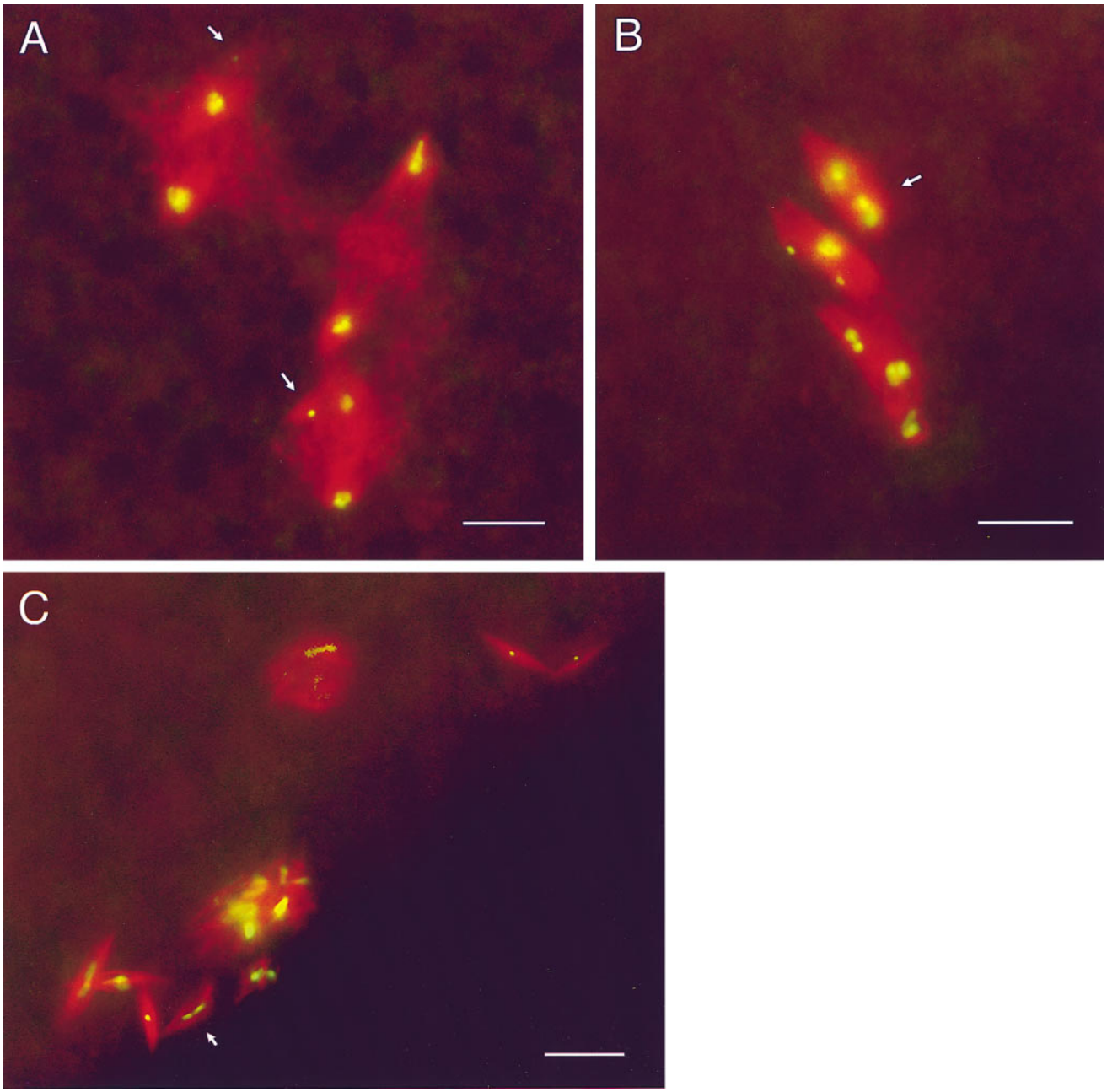

Figure 8. Meiotic divisions in normally activated fixed *ncd*^{2}*–gfp** mutant eggs. Normally oviposited mutant *ncd*^{2}*–gfp** eggs were fixed and stained with anti–α-tubulin antibody (*red*) and DAPI (*green*) to visualize the spindle microtubules and meiotic chromosomes. The cortex of the egg is nearer to the bottom of each of the images. (*A*) Late anaphase I half bivalents are segregating on separate spindles. The tiny fourth chromosomes (*arrows*) are associated with spindle spurs or small spindles. A hazy mass of tubulin-positive material is present in the central region of each spindle and is interpreted to be fragmented microtubules. The spindles at the top and bottom are bent or skewed, and the spindle in the middle is positioned obliquely with respect to the cortex. (*B*) Metaphase II chromosomes are associated with separate spindles or spindle spurs. The spindles are positioned obliquely or vertically (*arrow*) with respect to the cortex. The spindle indicated by the arrow is cross-sectioned and joined to a spindle spur with an associated chromosome. (*C*) Continued spindle-associated divisions of the maternal chromosomes after the initial two divisions. The egg contained 18 spindle-associated chromosomes or nondisjoined sister chromatids, more than the number of chromosomes expected after completion of the two meiotic divisions. Several of the chromosomes appear to be dividing. An anaphase chromosome configuration is indicated by the arrow. The spindles lack centrosomes and are present near the cortex, where the polar bodies are found in wild-type embryos. The egg was unfertilized and contained no mitotic spindles. Bars, 10 μm.

steps include the expansion/contraction of the spindle, spindle rotations, and the acute pivoting movement that reorients the spindle into a position perpendicular to the cortex before completion of the meiotic divisions.

Fusion of *ncd* to *gfp* and expression of the gene fusion in *Drosophila* under the control of the wild-type *ncd* promoter targets the fluorescent motor–GFP fusion protein to the meiotic spindle, permitting visualization of meiotic

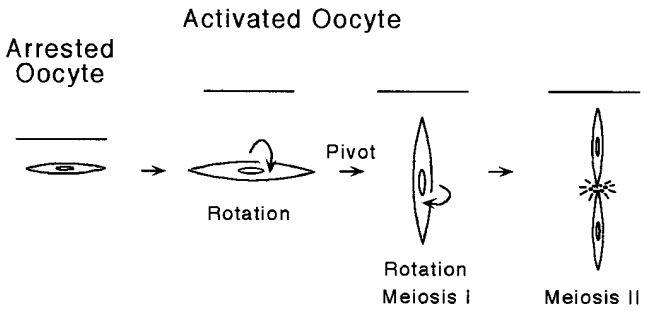

Figure 9. Model of spindle dynamics after oocyte activation. Meiosis I spindles in *Drosophila* oocytes are assembled parallel to the cortex of the oocyte (represented by the line) and remain in this position during metaphase arrest. After normal activation by ovulation, the oocyte swells. The spindle rotates around its long axis and pivots into a vertical position with respect to the cortex, followed by further rotations. Completion of meiosis I occurs with the spindle perpendicular to the cortex and is immediately followed by reorganization of the meiosis I spindle into two tandem meiosis II spindles and progression into meiosis II.

spindle dynamics in live oocytes. The Ncd–GFP fusion protein can replace the function of the wild-type Ncd motor protein, rescuing the *ca*nd null mutant both for chromosome segregation and embryo viability. Visualization of meiotic spindles using a microtubule-associated motor protein fused to GFP is a highly effective method for monitoring changes that occur in the oocyte spindle. The meiotic spindles can be visualized through the chorion of nonactivated or activated live oocytes, minimally perturbing the oocyte.

Meiosis I and II Spindle Dynamics in Wild-Type Oocytes

Spindles of nonactivated live oocytes were observed after dissection under oil, conditions that prevent oocyte hydration and consequent activation (Theurkauf, 1994). Most of the spindles were stable, showing only slight movements or changes in position over periods of 15–30 min observation. The spindles appeared to be undergoing dynamic changes, as evidenced by the detection of slight extensions/contractions in length and alternating clockwise and counter clockwise rotational movements. The spindles of nonactivated live oocytes were positioned parallel to the oocyte cortex and could be observed as early as stage 13 (King et al., 1956; Spradling, 1993) in oocytes that were still associated with degenerating nurse cells.

In contrast to the nonactivated live oocytes, live oocytes that were observed after brief immersion in *Drosophila* PBS contained spindles that were highly dynamic. The spindles extended and contracted, rotated around their long axis, and pivoted from their initial position parallel to the oocyte cortex into a vertical position, where they continued to rotate. We interpret the highly dynamic state of the meiotic spindle that we observe upon hydration of oocytes as representing the state of the spindle immediately after activation. The dynamic changes in the meiotic spindle after oocyte activation are shown schematically in the model in Fig. 9 and can be summarized as follows: (*a*) rotation of the spindle, (*b*) pivoting of the spindle vertical to the cortex, followed by rotations, (*c*) completion of meiosis I, and (*d*) assembly of meiosis II spindles and completion of meiosis II. Several of these changes can also be detected or observed in normally activated fixed eggs.

Rotation and pivoting of the *Drosophila* meiotic spindle have not been observed previously, although reorientation of the meiosis I spindle has been inferred to occur based on positional differences in spindles in metaphase-arrested and activated fixed oocytes (Riparbelli and Callaini, 1996). The rotations and acute pivoting movement of the spindle represent two of the initial changes that occur in the spindle after oocyte activation. The ability of the spindle to rotate and reorient before completing the meiotic divisions explains why the spindle in nonactivated live (Fig. 1) and fixed oocytes (Fig. 2; Theurkauf and Hawley, 1992; White-Cooper et al., 1993) can be observed parallel to the cortex, while the meiotic divisions occur with the spindle perpendicular to the cortex (Sonnenblick, 1950; Figs. 4 and 5). Our observations indicate that the meiotic spindle reorients soon after oocyte activation by an acute pivoting movement, accompanied by spindle rotations.

Upon reorientation perpendicular to the oocyte cortex, the spindles of in vitro–activated *Drosophila* oocytes frequently elongated and completed the meiosis I and then the meiosis II division. The transition into meiosis II after the completion of meiosis I, including assembly of the tandem meiosis II spindles, has not been observed previously, although the second meiotic division is known to occur with the two spindles tandemly aligned (Sonnenblick, 1950). The observations reported here indicate that assembly of the meiosis II spindles occurs by the formation of new spindle poles in the center of the anaphase I spindle, as anticipated by the work of others (Puro, 1991; Riparbelli and Callaini, 1996). The newly formed spindle poles serve as the central poles for the two meiosis II spindles. Assembly of the tandem meiosis II spindles appears to involve reorganization of the meiosis I spindle fibers, possibly by rapid sliding of the spindle microtubules, without disassembly of the meiosis I spindle.

The mechanism by which the central meiosis II spindle poles form is not known, although the ring- or disk-shaped central spindle pole body that lies between the two meiosis II spindles has been suggested to organize the poles (Puro, 1991). The recent observation that a centrosomal protein, CP190 (DMAP190), localizes to the central spindle pole body (Riparbelli and Callaini, 1996) suggests that centrosomal proteins are involved. In contrast, centrosomal proteins such as γ-tubulin, DMAP60, and DMAP190 have not been found associated with meiosis I spindles of *Drosophila* oocytes (Theurkauf and Hawley, 1992; Matthies et al., 1996). These observations raise the possibility that the mechanism by which spindle poles are formed for meiosis I and II spindle assembly in *Drosophila* oocytes differs, and that assembly of meiosis II spindles requires centrosomal proteins that are found in mitotically dividing cells.

Rotation of Meiotic Spindles in Xenopus Oocytes

In addition to the present work with *Drosophila*, meiotic spindle dynamics have been followed in activated live oocytes of *Xenopus* after injection of FITC-conjugated tubulin (Gard, 1992). The *Xenopus* meiosis I and II spindles as-

sembled with the long axis parallel to the oocyte surface and then rotated into a vertical position before undergoing division. Reorientation of the meiotic spindle in *Xenopus* oocytes was inhibited by treatment of oocytes with cytochalasin B during maturation (Gard et al., 1995), indicating the requirement for an intact actin cytoskeleton. Based on our present observations, meiosis I spindles of *Drosophila* and *Xenopus* oocytes undergo an analogous acute pivoting rotation before division. Division with the spindle perpendicular to the cortex positions one of the daughter nuclei more internally and the other closer to the surface. After completion of the second meiotic division, the innermost nucleus in *Drosophila* or the more internal nucleus in *Xenopus* becomes the female pronucleus, and the nuclei or nucleus near the cortex undergo polar body formation. The basis for the initial assembly of spindles parallel to the cortex is not certain, but may have to do with the anchoring or attachment of the spindle to the cortical actin cytoskeleton.

Despite their overall similarity, some aspects of spindle dynamics in *Xenopus* and *Drosophila* oocytes differ. For example, *Xenopus* meiotic spindles were not reported to rotate around their long axis before the acute pivoting rotation that reorients the spindle perpendicular to the cortex. The rotations of the *Drosophila* oocyte spindles may cause the pivoting and, after reorientation, lead to spindle elongation and completion of the meiotic divisions. The spindle pivotings in *Xenopus* and *Drosophila* could therefore be similar in effect, but differ in basis.

Oocyte Activation in Drosophila

The initial report of in vitro activation of *Drosophila* oocytes showed that hydration in hypotonic (diluted) Robb's medium (Robb, 1969) induces physiological changes in oocytes that are consistent with normal activation by ovulation (Mahowald et al., 1983). Tests of undiluted Robb's medium did not result in the ultrastructural changes typical of normally ovulated eggs that were also observed in oocytes treated with hypotonic medium. These results have led to the belief that hypotonic solution is required to activate oocytes. Activation by the criterion of completion of the meiotic divisions was apparently not tested in oocytes treated with undiluted medium. The Robb's medium used in this previous report was probably the chemically defined medium (Robb, 1969), which is similar in osmolarity and ionic composition to the *Drosophila* PBS developed at the same time (Robb, 1969), which was used in the present study.

Our observation that oocytes immersed briefly in undiluted *Drosophila* PBS undergo changes in the spindle that are consistent with activation, was therefore unexpected. The oocytes become visibly swollen upon immersion in the solution, resembling normally ovulated eggs, in contrast to nonactivated oocytes which appear wrinkled and shrunken. The oocytes treated with undiluted *Drosophila* PBS are activated by the criteria of re-entry into the meiotic cell cycle and completion of the meiotic divisions. Not all of the oocytes completed the meiotic divisions, however. Spindles in some oocytes reoriented perpendicular to the oocyte cortex and remained in this position for periods of 15–40-min observation, rotating around their long axis.

Perturbation of nonhydrated Drosophila oocytes can also cause activation, since 3/3 oocytes that were dissected under oil completed the meiotic divisions after their chorions were partially removed. Hydration of oocytes is therefore not required for activation. Activation of *ncd–gfp* oocytes using methods recently developed for efficient mass activation of *Drosophila* oocytes (Page and Orr-Weaver, 1997) may prove of value in future studies.

Effects of Loss of Ncd Function on Oocyte Meiotic Divisions

The classical mutant allele, ncd^2, shows loss of function based on its failure to rescue the ca^{nd} null mutant. The basis of the loss of function of ncd^2 is a missense mutation in a residue that forms part of the ATP-binding motif of Ncd: an ncd^2–*gfp** transgene containing the missense mutation but not the other three amino acid changes of ncd^2 causes mutant effects that parallel those of ncd^2. The $G_{446} \rightarrow R$ missense mutation of ncd^2 affects a glycine residue that is highly conserved among the kinesin proteins and located at the base of a loop, L5, on the surface of the Ncd motor domain in the crystal structure (Sablin et al., 1996). Together with two other surface loops, L5 forms the entry to the nucleotide-binding pocket of Ncd. Replacement of G_{446} with a positively charged arginine is likely to affect nucleotide binding or release from the motor, and alter the ability of the motor to bind to or dissociate from microtubules. This is expected to impair the ability of the motor to function in the spindle by causing defective movement on microtubules and/or aberrant crosslinking activity.

The Ncd^2–GFP* fusion protein is associated with meiotic spindle fibers in ncd^2–*gfp** mutant oocytes, as reported previously for Ncd^2 (Hatsumi and Endow, 1992*a*), but the meiotic spindles are abnormal. Previous reports (Hatsumi and Endow, 1992*b*; Matthies et al., 1996) have focused on Ncd and the assembly and stability of the meiosis I spindle in *Drosophila* oocytes. Based on the observation of multiple or multipolar spindles in mutant oocytes, the Ncd motor has been proposed to crosslink and move on the microtubules associated with the meiosis I chromosomes, forming a single bipolar spindle (Hatsumi and Endow, 1992*a*,*b*; Matthies et al., 1996). Analysis of live oocytes injected with rhodamine–tubulin to visualize meiotic spindles indicates that the Ncd motor is required for maintenance, as well as assembly, of bipolar meiosis I spindles (Matthies et al., 1996).

The present study focuses on spindle dynamics after oocyte activation. Our observations demonstrate that multipolar spindles are formed by separation of spindle poles upon oocyte activation in the presence of a loss-of-function Ncd motor. Wild-type Ncd is therefore required to maintain spindle pole integrity during the meiotic divisions, probably by crosslinking and moving on microtubules, preventing sliding forces from disrupting the spindle and separating the microtubule-associated chromosomes from one another. Normal elongation of the meiosis I and II spindles was infrequently observed in *ncd* mutant oocytes, implying that the Ncd motor facilitates the microtubule sliding that is probably needed for spindle elongation and the rapid assembly of the meiosis II spindles in wild-type oocytes. Loss of Ncd function does not eliminate the ability of the central meiosis II spindle poles to form, but it is

probably the impaired ability of the spindle fibers to slide against one another that causes failure of the meiosis II spindles to assemble, resulting instead in the formation of short tripolar or multipolar spindles.

Sliding of spindle microtubules against one another has been proposed previously to contribute to poleward translocation, or flux, of microtubules in mitosis that may underlie poleward movement of chromosomes (Mitchison, 1989). Microtubule polymerization/depolymerization and microtubule motors are both thought to produce forces that result in poleward microtubule flux (Mitchison and Salmon, 1992). The observations reported here indicate that microtubule sliding is an important aspect of meiotic spindle dynamics as well as the dynamics of mitotic spindles, and is probably facilitated by the Ncd microtubule motor.

In addition to defective spindle elongation and meiosis II spindle assembly, the spindle microtubules appear to be destabilized in *ncd*^{2}*–gfp** mutant oocytes. Fragmentation of spindle microtubules was observed in activated live *ncd*^{2}*–gfp** mutant oocytes, but not in activated live *ncd–gfp* or *ncd–gfp** oocytes. Fluorescent particles, probably microtubule fragments bound to Ncd^2–GFP*, were associated with depolymerizing spindle fibers of *ncd*^{2}*–gfp**, forming a hazy network in the center of the meiotic spindles, where the more unstable microtubule plus ends are expected to lie. Normally activated fixed *ncd*^{2}*–gfp** mutant eggs, stained with α-tubulin antibody to visualize microtubules, also showed a hazy mass of tubulin-positive fragments in the central regions of the meiosis I or II spindles, which was not observed in normally activated wild-type eggs fixed and stained with α-tubulin antibody. These observations indicate that the mutant Ncd^2–GFP* motor causes destabilization of spindle fibers and imply that wild-type Ncd functions to stabilize spindle fibers during completion of the meiotic divisions. Destabilization of microtubules by Ncd^2–GFP* could be due to altered ability of the mutant motor to bind to and move on microtubules, or to crosslink or bundle spindle fibers, as a consequence of the mutational change in its nucleotide binding site. It is also possible that Ncd^2–GFP* exhibits gain-of-function effects, based on its small semidominant effect on embryo viability. The implied role of Ncd in stabilizing microtubules therefore warrants substantiation by further evidence.

Dynamics of Spindle Pole Formation and the Ncd Microtubule Motor

A recent model for microtubule motor protein function in spindle pole formation invokes the ability of the motor both to crosslink microtubules and move along the crosslinked microtubules (Vernos and Karsenti, 1995). The proposed requirement for movement of the motor on the crosslinked microtubules is consistent with the cytological effects of the mutant Ncd^2–GFP* motor. Ncd^2 can bind to spindle microtubules and could also bundle them by interactions with its highly charged tail region (Chandra et al., 1993), but movement of the mutant motor on microtubules is probably impaired, as evidenced by its apparent inability to mediate microtubule sliding needed for spindle elongation. The proposed impaired ability of Ncd^2–GFP* to move on microtubules is correlated with the inability of the motor to maintain spindle poles, thus movement of the Ncd crosslinking activity along spindle microtubules is likely to be required to maintain spindle bipolarity.

Loss of Ncd function in *ncd*^{2}*–gfp** mutant oocytes causes misregulation of the meiotic divisions, resulting in continued divisions after the initial two divisions in in vitro–activated live mutant oocytes. Maternal chromosomes are also associated with spindles instead of the normal polar bodies in normally activated fixed mutant eggs. In wild-type embryos, the formation of polar bodies could sequester the maternal chromosomes from cytoplasmic factors, preventing further spindle-associated divisions. Loss of regulation over the number of meiotic divisions could be due to the inability of the mutant Ncd^2 motor to focus the meiotic chromosomes into polar bodies, which consist of chromosomes with centromeres oriented inward, surrounded by an array of short microtubules (Hatsumi and Endow, 1992*b*; Komma and Endow, 1997; Page and Orr-Weaver, 1997). The polar bodies of *Drosophila* resemble monopolar spindles and may undergo assembly in a manner similar to that of meiotic spindle poles. The apparent requirement for Ncd to focus the microtubule-associated chromosomes into polar bodies reinforces the idea that both crosslinking activity and movement of the crosslinking activity along microtubules are required to maintain focused arrays of microtubules such as spindle poles and polar bodies. Spindle-associated maternal chromosomes are also observed in embryos of the *ca*nd null mutant (Hatsumi and Endow, 1992*b*), evidence that the absence of Ncd, as well as the loss of Ncd function, results in continued divisions of the oocyte chromosomes.

Several effects of the loss of Ncd function that are reported here were not detected in previous studies of antibody-stained fixed oocytes and embryos. These include failure of meiosis I spindle elongation, failure of meiosis II spindle assembly, and destabilization of spindle fibers. The ability to monitor meiotic spindle dynamics in live oocytes provides an important means of determining the effect of mutants on spindle assembly and dynamics. Further studies should lead to a complete picture of the role of microtubule motors like Ncd, and microtubule dynamics, in meiotic spindle assembly and function.

Special thanks to T. Hazelrigg for *gfp–exu* DNA, a host stock for P element transformation, and helpful comments, and R. Tsien for the $S_{65} \rightarrow T$ mutant *gfp.* O.T. Hardy performed the in situ hybridization experiments to map the *ncd–gfp* and *ncd–gfp** insertions. We also thank W. Theurkauf for a protocol for preparation of nonactivated oocytes, W. Sullivan for a generous gift of rhodamine-conjugated anti–α-tubulin antibody, and W. Rasband for modification of NIH Image. The initial imaging of Ncd–GFP in oocytes was done with T. Salmon, who provided valuable guidance and suggestions.

This work is supported by grants from the National Institutes of Health and American Cancer Society to S.A. Endow.

Received for publication 18 February 1997 and in revised form 8 April 1997.

References

Chalfie, M., Y. Tu, G. Euskirchen, W.W. Ward, and D.C. Prasher. 1994. Green fluorescent protein as a marker for gene expression. *Science (Wash. DC).* 263:802–805.

Chandra, R., E.D. Salmon, H.P. Erickson, A. Lockhart, and S.A. Endow. 1993. Structural and functional domains of the *Drosophila* ncd microtubule motor protein. *J. Biol. Chem.* 268:9005–9013.

Doxsey, S.J., P. Stein, L. Evans, P.D. Calarco, and M. Kirschner. 1994. Pericen-

trin, a highly conserved centrosome protein involved in microtubule organization. *Cell.* 76:639–650.
Endow, S.A., and D.J. Komma. 1996. Centrosome and spindle function of the *Drosophila* Ncd microtubule motor visualized in live embryos using Ncd-GFP fusion proteins. *J. Cell Sci.* 109:2429–2442.
Endow, S.A., and D.W. Piston. 1997. Methods and protocols. *In* GFP: Green Fluorescent Protein Strategies and Applications. M. Chalfie and S. Kain, editors. John Wiley & Sons Inc., New York. In press.
Endow, S.A., S. Henikoff, and L. Soler-Niedziela. 1990. Mediation of meiotic and early mitotic chromosome segregation in *Drosophila* by a protein related to kinesin. *Nature (Lond.).* 345:81–83.
Endow, S.A., R. Chandra, D.J. Komma, A.H. Yamamoto, and E.D. Salmon. 1994. Mutants of the *Drosophila* ncd microtubule motor protein cause centrosomal and spindle pole defects in mitosis. *J. Cell Sci.* 107:859–867.
Gard, D.L. 1992. Microtubule organization during maturation of *Xenopus* oocytes: assembly and rotation of the meiotic spindles. *Dev. Biol.* 151:516–530.
Gard, D.L., B.-J. Cha, and A.D. Roeder. 1995. F-actin is required for spindle anchoring and rotation in *Xenopus* oocytes: a re-examination of the effects of cytochalasin B on oocyte maturation. *Zygote.* 3:17–26.
Gerhart, J.C. 1980. Mechanisms regulating pattern formation in the amphibian egg and early embryo. *In* Biological Regulation and Development. R.F. Goldberger, editor. Plenum Press, New York. 133–326.
Hatsumi, M., and S.A. Endow. 1992*a.* The *Drosophila* ncd microtubule motor protein is spindle-associated in meiotic and mitotic cells. *J. Cell Sci.* 103: 1013–1020.
Hatsumi, M., and S.A. Endow. 1992*b.* Mutants of the microtubule motor protein, nonclaret disjunctional, affect spindle structure and chromosome movement in meiosis and mitosis. *J. Cell Sci.* 101:547–559.
Heim, R., A.B. Cubitt, and R.Y. Tsien. 1995. Improved green fluorescence. *Nature (Lond.).* 373:663–664.
Kimble, M., and K. Church. 1983. Meiosis and early cleavage in *Drosophila melanogaster* eggs: effects of the claret-non-disjunctional mutation. *J. Cell Sci.* 62:301–318.
King, R.C., C. Rubinson, and R.F. Smith. 1956. Oogenesis in adult *Drosophila melanogaster. Growth.* 20:121–157.
Komma, D.J., and S.A. Endow. 1997. Enhancement of the ncd^D microtubule motor mutant by mutants of αTub67C. *J. Cell Sci.* 110:229–237.
Komma, D.J., A.S. Horne, and S.A. Endow. 1991. Separation of meiotic and mitotic effects of *claret nondisjunctional* on chromosome segregation in *Drosophila. EMBO (Eur. Mol. Biol. Organ.) J.* 10:419–424.
Lewis, E.B., and W. Gencarella. 1952. Claret and non-disjunction in *Drosophila melanogaster. Genetics.* 37:600–601.
Lindsley, D.L., and G.G. Zimm. 1992. The Genome of *Drosophila melanogaster.* Academic Press, Inc., San Diego, CA.
Mahowald, A.P., T.J. Goralski, and J.H. Caulton. 1983. *In vitro* activation of *Drosophila* eggs. *Dev. Biol.* 98:437–445.
Matthies, H.J.G., H.B. McDonald, L.S.B. Goldstein, and W.E. Theurkauf. 1996. Anastral meiotic spindle morphogenesis: role of the Non-Claret Disjunctional kinesin-like protein. *J. Cell Biol.* 134:455–464.
McDonald, H.B., and L.S.B. Goldstein. 1990. Identification and characterization of a gene encoding a kinesin-like protein in *Drosophila. Cell.* 61:991–1000.
McDonald, H.B., R.J. Stewart, and L.S.B. Goldstein. 1990. The kinesin-like *ncd* protein of *Drosophila* is a minus end-directed microtubule motor. *Cell.* 63: 1159–1165.
Mitchison, T.J. 1989. Polewards microtubule flux in the mitotic spindle: evidence from photoactivation of fluorescence. *J. Cell Biol.* 109:637–652.
Mitchison, T.J., and E.D. Salmon. 1992. Poleward kinetochore fiber movement occurs during both metaphase and anaphase-A in newt lung cell mitosis. *J. Cell Biol.* 119:569–582.
O'Tousa, J., and P. Szauter. 1980. The initial characterization of non-claret disjunctional (ncd): evidence that ca^{nd} is the double mutant, ca ncd. *Dros. Inf. Serv.* 55:119.
Page, A.W., and T.L. Orr-Weaver. 1997. Activation of the meiotic divisions in *Drosophila* oocytes. *Dev. Biol.* 183:195–207.
Pirrotta, V. 1988. Vectors for P-mediated transformation in *Drosophila. In* Vectors, A Survey of Molecular Cloning Vectors and Their Uses. R.L. Rodriguez and D.T. Denhardt, editors. Butterworth, Boston, MA. 437–456.
Prasher, D.C., V.K. Eckenrode, W.W. Ward, F.G. Prendergast, and M.J. Cormier. 1992. Primary structure of the *Aequorea victoria* green-fluorescent protein. *Gene (Amst.).* 111:229–233.
Puro, J. 1991. Differential mechanisms governing segregation of a univalent in oocytes and spermatocytes of *Drosophila melanogaster. Chromosoma (Berl.).* 100:305–314.
Riparbelli, M.G., and G. Callaini. 1996. Meiotic spindle organization in fertilized *Drosophila* oocyte: presence of centrosomal components in the meiotic apparatus. *J. Cell Sci.* 109:911–918.
Robb, J.A. 1969. Maintenance of imaginal discs of Drosophila melanogaster in chemically defined media. *J. Cell Biol.* 41:876–885.
Sablin, E.P., F.J. Kull, R. Cooke, R.D. Vale, and R.J. Fletterick. 1996. Crystal structure of the motor domain of the kinesin-related motor ncd. *Nature (Lond.).* 380:555–559.
Sonnenblick, B.P. 1950. The early embryology of Drosophila melanogaster. *In* Biology of Drosophila. M. Demerec, editor. Hafner Publication Co., New York. 62–167.
Spradling, A.C. 1993. Developmental genetics of oogenesis. *In* The Development of *Drosophila melanogaster.* Vol. 1. M. Bate and A. Martinez-Arias, editors. Cold Spring Harbor Laboratory, Cold Spring Harbor, New York. 1–70.
Stearns, T., L. Evans, and M. Kirschner. 1991. γ-tubulin is a highly conserved component of the centrosome. *Cell.* 65:825–836.
Sturtevant, A.H. 1929. The claret mutant type of *Drosophila simulans*: a study of chromosome elimination and of cell-lineage. *Z. Wiss. Zool.* 135:323–356.
Szollosi, D., P. Calarco, and R.P. Donahue. 1972. Absence of centrioles in the first and second meiotic spindles of mouse oocytes. *J. Cell Sci.* 11:521–541.
Theurkauf, W.E. 1994. Premature microtubule-dependent cytoplasmic streaming in *cappuccino* and *spire* mutant oocytes. *Science (Wash. DC).* 265:2093–2096.
Theurkauf, W.E., and R.S. Hawley. 1992. Meiotic spindle assembly in *Drosophila* females: behavior of nonexchange chromosomes and the effects of mutations in the nod kinesin-like protein. *J. Cell Biol.* 116:1167–1180.
Thummel, C.S., A.M. Boulet, and H.D. Lipshitz. 1988. Vectors for *Drosophila* P-element-mediated transformation and tissue culture transfection. *Gene.* 74:445–456.
Vernos, I., and E. Karsenti. 1995. Chromosomes take the lead in spindle assembly. *Trends Cell Biol.* 5:297–301.
Walczak, C.E., and T.J. Mitchison. 1996. Kinesin-related proteins at mitotic spindle poles: function and regulation. *Cell.* 85:943–946.
Wald, H. 1936. Cytologic studies on the abnormal development of the eggs of the claret mutant type of *Drosophila* simulans. *Genetics.* 21:264–281.
Walker, R.A., E.D. Salmon, and S.A. Endow. 1990. The *Drosophila claret* segregation protein is a minus-end directed motor molecule. *Nature (Lond.).* 347:780–782.
Wang, S., and T. Hazelrigg. 1994. Implications for *bcd* mRNA localization from spatial distribution of *exu* protein in Drosophila oogenesis. *Nature (Lond.).* 369:400–403.
White-Cooper, H., L. Alphey, and D.M. Glover. 1993. The *cdc25* homologue *twine* is required for only some aspects of the entry into meiosis in *Drosophila. J. Cell Sci.* 106:1035–1044.
Williams, B.C., T.L. Karr, J.M. Montgomery, and M.L. Goldberg. 1992. The *Drosophila l(1)zw10* gene product, required for accurate mitotic chromosome segregation, is redistributed at anaphase onset. *J. Cell Biol.* 118:759–773.
Yamamoto, A.H., D.J. Komma, C.D. Shaffer, V. Pirrotta, and S.A. Endow. 1989. The *claret* locus in *Drosophila* encodes products required for eyecolor and for meiotic chromosome segregation. *EMBO J.* 8:3543–3552.